Regulation of balanced root fungal community of *Vanda falcata* (Orchidaceae) by partitioning its mycorrhizal fungi and ascomycetous fungi across growth and development

Running title: *Vanda-Ceratobasidium* association

Galih Chersy Pujasatria[1], Ikuo Nishiguchi[2], Chihiro Miura[3], Masahide Yamato[4], and Hironori Kaminaka[3, *]

[1] The United Graduate School of Agricultural Science, Tottori University, Tottori 680-8553, Japan

[2] Suzuka city, Mie 510-0226, Japan

[3] Faculty of Agriculture, Tottori University, Tottori 680-8553, Japan

[4] Faculty of Education, Chiba University, Chiba 263-8522, Japan

[*] Corresponding author

Corresponding Author:

Hironori Kaminaka

Tel: +81-857-31-5378

E-mail: kaminaka@tottori-u.ac.jp

23 **ORCID**

24 Galih Chersy Pujasatria: https://orcid.org/0000-0002-2768-8250

25 Masahide Yamato: https://orcid.org/0000-0003-2238-4044

26 Hironori Kaminaka: https://orcid.org/0000-0002-3685-8688

27

28

Abstract

Epiphytic orchids are commonly found in exposed environments, which plausibly lead to different root fungal community structures from terrestrial orchids. Until recently, no studies have been conducted to show the fungal community structure during the growth of a photosynthetic and epiphytic orchid in its natural growing state. In this study, the *Vanda falcata* (commonly known as *Neofinetia falcata*), one of Japan's ornamental orchids, was used to characterize the fungal community structure at different developmental stages. Amplicon sequencing analysis showed that all development stages contain a similar fungal community: Ascomycota dominates half of the community while one-third of the community is Basidiomycota. *Rhizoctonia*-like fungi, a term to group the most common basidiomycetous fungi that form orchid mycorrhiza, exist even in a smaller portion (around a quarter) compared to other Basidiomycota members. While ascomycetous fungi exhibit pathogenicity, two *Ceratobasidium* strains isolated from young and adult plants could initiate seed germination *in vitro*. It was also found that the colonization of mycorrhizal fungi was concentrated in the lower part of the root where it directly attaches to the phorophyte bark, while ascomycetous fungi were distributed in the velamen but never colonized cortical cells. Additionally, lower root parts attached to the bark have denser exodermal passage cells, and these cells were colonized only by mycorrhizal fungi that further infiltrated the cortical area. Therefore, we propose that physical regulation of fungal entry to partition the ascomycetes and mycorrhizal fungi results in the balanced mycorrhizal symbiosis in this orchid.

(243 words)

Keywords: *Ceratobasidium*, epiphytic orchid, fungal microbiome, microbial dynamics, symbiotic germination, *Vanda falcata*

Introduction

Orchidaceae, one of the biggest flowering plant families, is widely distributed in almost all parts of the world. However, many orchid species are listed as endangered owing to habitat degradation and dependence on other organisms, i.e., pollinators (Suetsugu et al. 2015; Freitas et al. 2020). Moreover, establishing orchids in the natural habitat is always complicated, even in suitable conditions (Pujasatria et al. 2020). Due to its unique, one-of-a-kind traits, orchid seed germination is often hard to occur naturally. Despite extremely high fecundity, endosperm in orchids' seeds is almost absent. Consequently, orchids' seeds are nearly impossible to germinate without nutritional support. For seeds to successfully germinate and grow into mature plants, they must establish orchid mycorrhizal (OM) symbiosis (Arditti and Ghani 2000; Barthlott et al. 2014; Yeh et al. 2019; Pujasatria et al. 2020). Colonization of orchid mycorrhizal fungi (OMF) starts at seed germination and may last until adulthood. As with other mycorrhizae, OMF forms coiled hyphae in its host cells. This structure is termed peloton, where the exchange of nutrients (e.g., carbon, nitrogen, and phosphorus) occurs (Yeh et al. 2019). However, OM is unique because the host eventually digests the pelotons for further nutrient acquisition (Kuga et al. 2014). Based on this, orchids are considered parasitizing the fungus. This behavior, termed mycoheterotrophy, occurs mostly during the early growth stage where protocorms are still achlorophyllous and may continue until adulthood in various genera (Rasmussen et al. 2015; Yeh et al. 2019).

Most orchids associate with *Rhizoctonia*-like fungi, a broad term for several genera resembling the anamorphic morphology of *Rhizoctonia*. As symbionts, there are three genera in this group: *Ceratobasidium, Serendipita* (often associated with *Sebacina sensu lato*), and *Tulasnella* (Rasmussen et al. 2015; Yeh et al. 2019; Pujasatria et al. 2020). Originally, those fungi are saprophytic, endophytic, or even pathogenic. However, among

those genera, many species were isolated from orchid roots and proved to be mycorrhizal upon co-inoculation with seeds of respective orchid species (Pujasatria et al. 2020).

Studies on OMF of epiphytic orchids are lacking despite their vast diversity, compared to terrestrial orchids (Yukawa et al. 2009). While the roots of terrestrial orchids are usually subterranean, epiphytic orchids are commonly found growing in exposed environments and are prone to desiccation due to weather change (Rachanarin et al. 2018; Freitas et al. 2020). This leads to a presumably different fungal community compared to those of the underground. Microclimate change and phorophyte architecture also affect the establishment of epiphytic orchids (Rasmussen and Rasmussen 2018), especially for those living in a fluctuating climate, such as temperate regions. The availability of OMF on a particular substrate–in this case, arboreal–is also dependent on such a microenvironment since fungus intrinsically prefers unexposed, moist conditions to grow. When orchid seed lands on the substrate, its germination is not guaranteed since colonization of appropriate OMF is required. Thus, the interaction between 'the orchid and the fungal community would be important during the orchid's establishment and growth.

Most epiphytic orchids studied tend to associate with either *Ceratobasidium* or *Tulasnella* (Yukawa et al. 2009; Zettler et al. 2013; Rachanarin et al. 2018; Pujasatria et al. 2020; Freitas et al. 2020). However, more specifically, studies on OMFs of monopodial epiphytic orchids are limited. Several studies were already conducted on angraecoids (Hoang et al. 2017; Kendon et al. 2020), either leafy or aphyllous, but still limited to vandaceous (Carlsward et al. 2006).

This study focused on *Vanda* (syn. *Neofinetia*) *falcata*. This epiphytic orchid is known as one of Japan's ornamental orchids. Naturally, this orchid is distributed across central to southern Japan and reportedly grows on evergreen or deciduous trees (Suetsugu et al. 2015).

Unlike typical epiphytic orchids concentrated in tropical regions, *V. falcata* is adapted to subtropic and to the temperate areas, which may affect its association with fungi on phorophytes. Previous studies suggested that vandaceous orchids–especially those of subtribe Aeridinae–mainly associated with *Ceratobasidium*, proven by metabarcoding and seed germination results (Otero et al. 2002; Yukawa et al. 2009; Hoang et al. 2017; Mújica et al. 2018; Rammitsu et al. 2019; Kendon et al. 2020). Although *Ceratobasidium* strains have also been isolated from *V. falcata* (Rammitsu et al. 2021), mycobionts for seed germination have never been reported. Thus, this study analyzed the whole fungal community in seeds and root samples of *V. falcata* using amplicon sequencing. Additionally, pure fungal cultures were isolated from the same root pieces. Based on microscopic and molecular analysis, it was found that some of the isolated fungi were *Rhizoctonia*-like fungi. Finally, co-inoculation experiment was conducted to determine the interaction of these fungi for their colonization with seeds and roots of *V. falcata*.

Materials and Methods

Plant materials

Vanda falcata plants growing on a persimmon (*Diospyros kaki*) trunk were obtained from Kihoku Town, Mie Prefecture, Japan (34°06'27" N, 136°14'17" E). The residents eventually cut the trunk due to safety reasons, and it was maintained in Suzuka City of the same prefecture (34°51'05" N, 136°36'123" E) (Fig. 1A). Roots of young (small to medium plants that never flowered) and adult (those already flowered at least once) plants (Fig. 1B, C) attached to bark were randomly collected, and the harvested samples were stored at 4°C until use. The baiting method assessed fungal diversity inside the seeds: 3 x 6 cm nylon mesh packs containing ca. 100 *V. falcata* seeds were tied adjacent to twelve randomly selected

plants, including young and adult plants. The baiting method was conducted during spring (March–June 2020). The seeds and young/adult plant roots were surface sterilized and stored in 70% ethanol at 4°C until DNA extraction.

DNA extraction from plant materials and amplicon sequencing

Seeds isolated from the baiting method and root segments of randomly selected young and adult plants were used as materials for DNA extraction using the Real Genomics Plant DNA Extraction kit (RBC Bioscience, Taipei, Taiwan). After extraction, DNA concentration was measured using DS-11 spectrophotometer (DeNovix, DW, USA). The internal transcribed spacer (ITS) region was amplified using ITS1F_KYO1/ITS2_KYO2 for ITS1 and a pair of gITS/ITS4 for ITS2 (Ihrmark et al. 2012; Toju et al. 2012) (Table S1). Each reaction mixture (20-µl) contains 1-ng genomic DNA, 1-µl of 20-µM primer forward/reverse, and 10-µl KOD One PCR Master Mix (Toyobo, Osaka, Japan). For amplification, PCR was coonducted on T100 thermal cycler (Bio-Rad, CA, USA) using the following program: initial denaturation at 94°C for two minutes, 94°C for 30 secs, followed by 25 cycles of 50°C for 30 secs, 72°C for one minute, and final elongation step at 72°C for seven minutes. PCR results were confirmed using 1% (w/v) agarose gel electrophoresis. The sequencing of libraries prepared by PCR with barcode-containing primers using Illumina MiSeq platform (2 × 300 bp) and data analysis was conducted by the Bioengineering Lab Co., Ltd. (Atsugi, Japan). The raw sequence data obtained as fastq file was processed using the FASTX toolkit v0.0.13 (Hannon 2010) and Sickle v1.33 (Joshi and Fass 2011) to remove adaptor and primer sequences, ambiguous reads, low-quality sequences (quality score less than Q20), and reads no more than 40-bp. Quality-filtered sequences were merged using FLASH v1.12.11 (Magoč and Salzberg 2011) and used for the production of the representative sequences and operational taxonomic

unit (OTU) table using Qiime2 (v2020.6) (Bolyen et al. 2019) after removing the illusion and noise sequences using dada2 plugin. The representative sequences were compared to OTUs (97%) in UNITE v8.2 (Nilsson et al. 2019) to classify by taxon using the fitted classifier of Qiime2. Additionally, alpha and beta diversity analyses were conducted using Qiime2 diversity plugin.

Amplicon sequencing results were visualized using RStudio v4.0.2. The *ggpubr* package was used to visualize fungal diversity indices (OTU abundance, Chao1, Pielou, and Shannon Evenness Index/SEI), and the proportion of each fungal phylum observed in samples (Kassambara 2018). Principal coordinate analysis (PCoA) plots–based on Bray-Curtis index, Euclidean distance, and without any data transformations–were visualized using the *vegan* package (Oksanen et al. 2007). Additionally, analysis of similarity (ANOSIM) was used to calculate PCoA statistical significance ($p < 0.05$), using the same package.

Fungi-colonized root morphology observation

Crossing manual sections of fungi-colonized root were stained using 3% (w/v) acid fuchsin in glacial acetic acid (Gange et al. 1999) or UV autofluorescence after clearing in 10% KOH for one hour at 90°C to observe the presence of OMF and other fungi. The samples were then observed under a light microscope (BX53; Olympus, Tokyo, Japan), and images were taken using the equipped digital camera (DP27; Olympus). Statistics for quantification of OMF colonization in roots was calculated using ANOVA based on the results of the Kolmogorov-Smirnov normality test and Bartlett test using *ggpubr* package of RStudio v4.0.2 (Kassambara 2018). Subsequent Tukey *post hoc* test was conducted using the same software.

Rhizoctonia-like and pathogenic fungi isolation

Roots of young and adult plants were sectioned manually and observed using light (BX53) or stereo microscope (SZX16; Olympus). Subsequently, root sections with fungal colonization in cortex were put on either potato dextrose agar (PDA), one-sixth strength Czapek-Dox agar, or Fungal Isolation Medium (Zettler et al. 2013) supplemented with 10-µg/mL tetracycline. Fungi with *Rhizoctonia*-like characteristics (Oberwinkler et al. 2013; Weiß et al. 2016) were cultured on PDA, malt extract agar (MA), full-strength V8 juice agar (V8), or oatmeal agar (OMA) media at 25°C, and then stored at 4°C for long-term storage, while all non-*Rhizoctonia*-like fungi were cultured only on OMA at 25°C. Hyphae were stained using 0.01% ethidium bromide in 25% ethanol (Singh and Kumar 1991), and the cell wall was stained using a mixture of 1-mg/L calcofluor white and 0.5-mg/L Evans blue, to count the nuclei of *Rhizoctonia*-like fungal hyphae. Samples were observed under a fluorescence microscope (DM2500; Leica, Wetzlar, Germany) equipped with a digital camera (DFC310 FX; Leica) and visualized using ImageJ v.1.53a.

Fungal genomic DNA was extracted from the cultured fungi using the sorbitol-cetrimonium bromide (CTAB) combination method (Inglis et al. 2018). After extraction, DNA concentration was measured as described above. The ITS region was amplified using a combination of ITS1OF/ITS4 (Table S1) (Taylor and McCormick 2008; Toju et al. 2012). The PCR mixture for each sample contains 1-µl fungal genomic DNA, 1-µl of 20-µM primer forward/reverse, and 10-µl GoTaq Green Master Mix (Promega, WI, USA). Amplification was conducted using the following program: initial denaturation at 95°C for ten minutes, followed by 35 cycles at 95°C for 20 secs, 50°C for 30 secs, 72°C for 20 secs, and a final elongation step at 72°C for seven minutes. Successfully amplified DNA fragments confirmed by 1% (w/v) agarose gel electrophoresis were cloned using TOPO TA Cloning Kit

(ThermoFischer Scientific, MA, USA) and sequenced using Sanger method with both M13 forward and reverse primers by Eurofins Genomics (Tokyo, Japan). DNA sequences were subjected to BLAST (https://blast.ncbi.nlm.nih.gov/Blast.cgi) to identify the closest taxa.

Phylogenetic analysis

Fungal ITS DNA sequences were aligned using ClustalW v1.6, and subsequent maximum likelihood (ML) phylogenetic tree construction was conducted using RAxML-HPC v8.2.10 implemented in GENETYX-Windows v15 (Genetyx, Tokyo, Japan) with GTRGAMMA model and 1000 bootstrap analysis to infer the phylogenetic position of fungal OTUs and isolated strains of *Rhizoctonia*-like fungi. The best rooted tree was visualized using Iroki online tool (Moore et al. 2020).

In vitro seed germination assay

Eleven *Rhizoctonia*-like fungal strains containing *Ceratobasidium, Serendipita,* and *Tulasnella* (Table 1), obtained from culture stock centers, ATCC (American Type Culture Collection), RIKEN bioresource center (JCM strain), NARO Genebank (MAFF strains) and NITE biological resource center (NBRC strains), were inoculated on OMA for two weeks before symbiotic germination assay. Dehiscent capsules formed from naturally pollinated flowers were used to obtain the *V. falcata* seeds. Seeds were sterilized using 3% hydrogen peroxide and washed two to three times with sterilized water. Cultures were stored at 25°C for eight weeks in darkness. Germination stage description (Zettler et al. 2007) was modified according to the preliminary germination assay result (Table 2, Fig. S1). Protocorm growth index (GI) was evaluated using the equation $GI = \sum_{i=5}^{n} i(S_i) / \sum S$, with i; germination stage number (starting from stage 0 to 5), n; total seeds in one treatment, and n_i; total seeds

reaching germination stage *i* (Guimarães et al. 2013), and symbiotic cells were counted after six weeks. Each fungal treatment was replicated four times, with each plate containing ca. 100–300 seeds. Additionally, two ascomycetous fungi isolated from roots, *Pyrenochaetopsis* and *Fusarium,* were also subjected to similar germination assay to observe their interaction with seeds (Table 3). Protocorms were stained using 1-g/L calcofluor white counterstained with 0.5-g/L Evans blue, and fungal hyphae were stained using 1-mg/L WGA-Alexa Fluor 594 (ThermoFisher Scientific). Visualization was conducted using a fluorescent microscope (DM2500) equipped with a digital camera (DFC310 FX) and ImageJ v.1.53a, while symbiotic cells were counted using a tally counter from 25 randomly selected protocorms. Based on the results of the Kolmogorov-Smirnov normality test and Bartlett test, the Kruskal–Wallis test was conducted using *ggpubr* package of RStudio v4.0.2 (Kassambara 2018). Subsequently, Dunn's *post hoc* test with Benjamini-Hochberg false discovery rate adjustment ($p < 0.05$) was conducted using the *FSA* package of the same software (Ogle et al. 2021).

Results

Amplicon sequencing

Genomic DNA was obtained from three kinds of samples: seeds, roots of young plants, and roots of adult plants. The seeds were taken from twelve seed packs and combined as one even though no germinating seeds were found. For root samples, three to four root sections (ca. 5-cm each) were cut from a young or adult plant. In root samples, the most conspicuous feature of the symbiotic region was a yellowish root surface that contains digested pelotons (Fig. 1D). This was primarily obvious when the roots were wet. This coloration is unique to the root parts directly attached to *D. kaki* bark (Fig. 1E).

The ITS1 and ITS2 PCR products were subjected to amplicon sequencing by Illumina MiSeq. Each sample sequencing generated 36,027 to 72,301 raw reads for ITS1 and 40,033 to 72,014 raw reads for ITS2. 83% and 89.47% of the whole reads were processed and used for further analysis (Table S2). Phylogenetic OTUs were generated at 97% similarity cutoff using Qiime2 and ranged from 155 to 411 OTUs for each sample in ITS1 and 174 to 476 OTUs for each sample in ITS2 (Table S3, S4). In total, 1274 and 1358 phylogenetic OTUs were obtained for ITS1 and ITS2, respectively.

General fungal diversity and OMF localization in roots

PCoA results conducted using generated OTUs from both ITS sequenced data showed distinct groupings of fungal communities among the three development stages–seed, young plant, and adult plant (Fig. 2), but ANOSIM did not give a significant result for ITS2 ($p < 0.05$). R-value of 0.3913 (sig. = 0.0419) for ITS1 and 0.2047 (sig. = 0.1965) for ITS2 shows that the fungal compositions between the stages were not distinguished (Clarke 1993) (Fig. 2). R-value between ITS1 and ITS2 communities has different significance level but both values imply that the degree of discrimination is not changed. The community structure similarities were also supported by Pielou evenness (J') and SEI, where fungal diversity in all samples was not significantly different (Fig. S2). Ascomycota and Basidiomycota were the most prevalent phyla at the phylum level, with coverage of above 50% in each sample (Fig. S3). The other phyla were Chytridiomycota, Mortierellomycota, and Mucoromycota, which were found in smaller amounts.

In *Rhizoctonia*-like fungi, *Ceratobasidium* was found in trace amounts in seed samples but was unexpectedly found only in one young root sample. It was also found in two other adult root samples but only in trace amounts. Another similar case is in *Serendipita*, which

was relatively abundant only in seed samples. *Tulasnella* was very limited in seed samples but gradually increased in young and adult root samples (Fig. 3A, S4). Thus, while the whole fungal community did not alter, existence of *Rhizoctonia*-like fungi (*Ceratobasidium, Serendipita,* and *Tulasnella*) tended to change over time following the growth and development of *V. falcata.*

Both ITS sequences exhibited relatively similar diversity indices. However, ITS2 has been considered a suitable marker for revealing the operational taxonomic richness and taxonomy specifics of fungal communities due to the broader taxonomic information (Yang et al. 2018). Therefore, this study mainly focused on the ITS2 sequences in subsequent analysis.

Identification of Rhizoctonia-like fungal OTUs

Among all basidiomycetous fungal sequences, fourteen OTUs annotated as Rhizoctonia-like genera (Table S5) were extracted for the heatmap diagram (Fig. 3A). ML phylogenetic trees based on the representative sequences of each OTU were constructed to see whether the fungi belong to a particular OMF species in their respective families (Fig. 3B). Five *Ceratobasidium* OTUs (accession numbers LC602782–LC602785) were closely related to a mycobiont of epiphytic orchid *Taeniophyllum glandulosum* isolated in Japan (LC405936) (Rammitsu et al. 2019). Six *Serendipita* OTUs (LC602788–LC602792) assigned to Sebacinaceae were divided into two clades inside Serendipitaceae: two OTUs were related to *Serendipita herbamans* (NR144842), an endophyte of *Bistorta vivipara* (Polygonaceae) (Riess et al. 2014) in one clade, and the other four OTUs were close to *S. indica* (NR166023, KF061284, MH863568), a well-known endophyte occurring in several flowering plants (Weiß et al. 2016). Two *Tulasnella* OTUs (LC602793 and LC602794) were related to *T. irregularis* (EU218889) and *T. amonilioides* (JF907601 and JF907599), mycobionts first

reported in *Dendrobium affine* (syn. *dicuphum*) and *Encyclia dichroma*, respectively (Warcup and Talbot 1980; Almeida et al. 2014).

Isolation of Rhizoctonia-like fungi from plant samples

We initially attempted to isolate pure fungal cultures from all samples (seeds, protocorms, and roots) to verify that *V. falcata* associated with *Rhizoctonia*-like fungus during the development *in situ*. However, since no germinating seeds were found, roots of randomly selected young and adult plants were only used for the fungal isolation. We could only isolate two pure isolates of *Rhizoctonia*-like fungi from these root sections despite more than 30 attempts, including those with conspicuous symbiotic regions. We faced two major challenges to obtain a pure culture, which include: (1) most pelotons were already digested, and (2) other endophytic ascomycetous fungi–mostly those morphologically resembling *Trichoderma*, *Cladosporium*, or *Phoma*–often outgrew preferred *Rhizoctonia*-like fungi in the isolation media. In root samples, ascomycetous fungi were found in the epidermis with its conidial form (Fig. 4A). Based on the conidia structure, some of these fungi were identified as *Lasiodiplodia* and Pleosporales (Zhang et al. 2012). However, upon further examination into exodermis, no fungi colonized the exodermal cells. Instead, *Rhizoctonia*-like fungi formed peloton in exodermal passage cells. Based on hyphal morphology, it resembles *Rhizoctonia*-like fungus isolated from roots: both possess hyphae with irregular width, commonly called monilioid hyphae (Fig. 4B, S5). Upon forming peloton inside passage cells, the *Rhizoctonia*-like fungi infiltrate cortical cells to form the peloton network. Additionally, passage cells are concentrated in lower part of the root. Following this, OMF is also mostly found in the same part (Fig. 4C).

315 The isolated *Rhizoctonia*-like fungi were named BI-103P from young and DE-52P
316 from the adult plant root segments (Table 3, Fig. S6A, B). Morphologically, those fungal
317 strains followed common descriptions for *Rhizoctonia*: branching at a right angle, constriction
318 of hyphae at the site of branching, occasionally visible dolipore septa, and septation at a short
319 distance after branching (Ogoshi 1975). The ITS sequences of these isolates were subjected to
320 pairwise DNA alignment, a feature of Mycobank (https://www.mycobank.org/) and BLAST,
321 which revealed that both strains belong to Ceratobasidiaceae. These strains were closest to
322 AB507066.1, an uncultured *Ceratobasidium* from another epiphytic orchid *Phalaenopsis* (syn.
323 *Sedirea*) *japonica* from Miyazaki Prefecture in southern Japan (Yukawa et al. 2009). We also
324 found that the hyphae are binucleate, indicating that these fungi are traditionally classified
325 into 'binucleate *Rhizoctonia'* (Fig. S6C, D).
326
327 *In vitro seed germination using isolated Ceratobasidium strains and Ascomycota fungi*
328 *V. falcata* seeds were used for symbiotic germination using isolated *Ceratobasidium* strains
329 and other *Rhizoctonia*-like fungi strains including *Serendipita* and *Tulasnella* obtained from
330 culture stock centers (Table 1). Seeds inoculated with compatible OMF started to undergo
331 imbibition and usually formed rhizoids upon entering stage 2 (Fig. S1A). Protocorms started
332 to turn greenish at the onset of stage 3, and shoot primordium was developed as an irregular
333 protrusion on the terminal part (Fig. S1B). This protrusion will eventually form a crest (Fig.
334 S1C). Compared to other stages, stage 4 protocorms were rarely observed. This stage is
335 characterized by the formation of the first leaf (Fig. S1C). Based on fluorescence imaging,
336 fungal colonization started from the suspensor and spread up to 75% of protocorm size (Fig.
337 S1D).

Based on the germination stage description summarized in Table 2, four of six Ceratobasidium strains (C. sp. BI (BI-103P), C. sp. DE (DE-52P), C. sp. TA1, and C. sp. TA2) yielded remarkably higher GI than others based on Kruskal-Wallis test ($p < 0.05$) (Fig. 5A). Following GI, symbiotic cell count also increased. Protocorms yielded from suitable fungal treatments also had a high symbiotic cell count (Fig. 5B). It was found that these four strains are included in the same phylogenetic clade (Fig. 6). However, few symbiotic cells were found in other Ceratobasidium, Serendipita, and Tulasnella treatments. These strains could only induce germination until stage 1 even after eight weeks. The protocorms kept swollen, but no pathogenic effect was observed, indicating that these strains simply did not further associate with protocorms, and the swelling was merely a result of imbibition. These results indicated that V. falcata seeds may have specificity toward a group of Ceratobasidium fungi.

During the process of isolating the *Rhizoctonia*-like fungi from root samples, two Ascomycota fungi *Pyrenochaetopsis* (NE-4) and *Fusarium* (MI-5) (Table 3), were also isolated and identified. Since these are known as pathogenic fungi, the effects of these non-*Rhizoctonia*-like fungi on *V. falcata* seeds were also analyzed using *in vitro* germination assay. At the early stage, seeds were swelling and colonized by *Pyrenochaetopsis* but eventually killed after pycnidia formation, indicated by the blackening of seeds (Fig. 7A). Similarly, the seeds sown on *Fusarium* were heavily colonized and were eventually degraded (Fig. 7B). These results suggested the importance of partitioning between ascomycetous and *Rhizoctonia*-like fungi inside the roots. Additionally, these ascomycetous fungi were incompatible with *V. falcata* seeds for germination.

Discussion

While most reports on mycorrhizal associations of the Vandeae tribe come from the Angraecinae subtribe (angraecoids), reports on the Aeridinae subtribe members are still minimal. This study focused on *V. falcata* fungal community structure of the three developmental stages, i.e., seeds, young plants, and adult plants. This study emphasizes this point to show how an orchid maintains its inner fungal community in each developmental stage. All observations provided several findings. Firstly, Ascomycota was the dominant phylum in all examined seeds, young plants, and adult plants. Secondly, ascomycetous, some of which are potential pathogenic fungi, colonized epidermal areas of *V. falcata* roots, while *Rhizoctonia*-like fungi (OMF) colonized the cortical area. Thirdly, *V. falcata* associates with a group of *Ceratobasidium* fungi for seed germination.

Although amplicon sequencing results are not thought to directly reflect fungal community outside samples (i.e., bark surface), the results suggest that the growing substrate does not necessarily provide suitable conditions for OM establishment in epiphytic orchids. Based on the information obtained from PCoA, it was shown that the fungal community in seeds, young, and adult plants were similar with slight differences. Ascomycetous fungal classes, such as Sordariomycetes, Dothideomycetes, and Leotiomycetes frequently occur in all samples, and most of the members are known to be saprobic or parasitic in several habitats, including tree surface where epiphytic orchids coexist (Schoch et al. 2009; Herrera et al. 2010). Seeds landing on bark become the potential hosts of these fungi, especially for *Rhizoctonia*-like fungi, present on the same site. Although it is unknown whether the proportion of ascomycetous and *Rhizoctonia*-like fungi on *D. kaki* bark is similar to that inside *V. falcata* seeds, in the end, ascomycetous fungi will be dominant in the seeds. Even if compatible *Rhizoctonia*-like fungus is present inside the seeds, ascomycetous fungi could encompass the seeds even before germination occurs. Severe infection of *Pyrenochaetopsis* and *Fusarium,*

386 which were isolated from healthy roots upon inoculation with these fungi, indicates that the
387 presence of ascomycetous fungi is a potential hinderance for *V. falcata* germination. As
388 with any endophytic relationship, there is a balanced state between endophyte and roots
389 where the endophyte inhabits within the root without damage to the root. However, when
390 the endophyte was grown on nutrient rich media, it may exhibit virulence against the host
391 (Sarsaiya et al. 2020). In this study, *V. falcata* seeds dispersed on the substrate was
392 vulnerable to *Pyrenochaetopsis* and *Fusarium*.

393 In the case of *Rhizoctonia*-like fungi, sequence reads in *Serendipita* OTUs were high in
394 seeds, but they much lower in young and adult roots. Conversely, little reads in *Tulasnella*
395 were found in seeds, but its occurrence increases in young and adult roots. The occurrence of
396 *Serendipita* OTUs compared to that of *Ceratobasidium* and *Tulasnella* in seeds indicates the
397 shifting of *Rhizoctonia*-like fungi preference during development but may not necessarily
398 reflect the actual OM association. If *Serendipita* is the OMF of *V. falcata*, seeds in baiting
399 samples should have germinated. Although the number of OTU sequences for *Serendipita*,
400 *Tulasnella*, and *Ceratobasidium* were different at each developmental stage as mentioned, the
401 function of these Rhizoctonia-like fungi is difficult to be speculated based only on the current
402 data and needs to be further investigated.

403 Among all fungi isolated from root sections, *Ceratobasidium* sp. BI and *C.* sp. DE from
404 young and adult plant roots were confirmed to associate with *V. falcata* due to their capability
405 to propagate seed germination. Interestingly, another strain *Ceratobasidium sp.* TA2 isolated
406 from an epiphytic orchid *Taeniophyllum glandulosum* in Shizuoka Prefecture (Rammitsu et al.
407 2019) induced better germination results. These three *Ceratobasidium* strains formed a similar
408 clade in the phylogenetic analysis. Therefore, it is suggested that *V. falcata* associates with a
409 narrow range of *Ceratobasidium* in seed germination. Associating with various fungi is

advantageous if the OMF occurrence is sporadic, which allows the orchid to readily develop with any compatible fungus available on each growing site (Xing et al. 2019). Generally, it is accepted that orchids with high mycorrhizal specificity are most likely to be rare due to high dependency on OMF distribution in their natural habitats. In the case of *V. falcata*, its distributions were constricted from central to southern Japan with various types of phorophytes (Suetsugu et al. 2015; Rammitsu et al. 2019, 2021). Accordingly, *V. falcata* has high phenotypic variation even for wild plants across Japan, causing such extensive association to be beneficial to the plant for distribution.

We propose that the partitioning of OMF and ascomycetous fungi protects the mycorrhizal root. In this study, ascomycetous fungi mainly detected in *V. falcata* roots were Sordariomycetes, Dothideomycetes, and Leotiomycetes, commonly known as saprobes and pathogens on tree bark (Naranjo-Ortiz and Gabaldón 2019). Primarily based on their saprobic nature, it is plausible that these fungi mainly colonize *D. kaki* bark, and through the orchid root-bark interface, these fungi further penetrate velamen. Although OMF can penetrate into cortical cells, invasion of the ascomycetous fungi is inhibited by exodermis, thus accumulating them inside velamen. Orchid roots typically contain exodermis with lignification of the tangential walls and smaller, non-lignified passage cells that allow OMF to penetrate the cortical cells (Esnault et al. 1994). It is also reported that the passage cell is related to OMF colonization; that is, the root part with denser passage cells has more OMF colonization (Chomicki et al. 2014). Based on these concepts, we also confirmed that passage cells exist in both root surfaces, those attached to bark and those exposed to the air, and the lower part attached to bark had dense passage cells, which was related to higher mycorrhizal colonization in this part. While passage cells are constantly available for OMF to infiltrate, the upper parts of the root mostly remain uncolonized. The exact explanations for this finding

434 are still lacking, but we suggest that chemical (deposition of phenolics, etc.) or environmental
435 (light exposure, etc.) factors might be included. Further studies on how internal and external
436 factors affect epiphytic root colonization by fungi are required to elaborate on this
437 phenomenon.
438
439 **Conclusions**
440 To sum up, *V. falcata's* fungal community structure is similar across growth development.
441 Ascomycota was the dominant phylum, while the others were found in a smaller amount,
442 even for *Rhizoctonia*-like fungi (Fig. 8). It was also confirmed that seeds of *V. falcata*
443 germinated in symbioses with *Ceratobasidium* isolated from its roots and another strain
444 isolated from another orchid. We also propose that the innate regulation of fungal entry also
445 causes this balanced fungal community and partitioning of ascomycetes as well as OMF.
446 Therefore, further studies on how root balances fungal colonization are required to decipher
447 this partitioning mechanism in *V. falcata* or any other epiphytic orchids.
448
449 **Data Accessibility**
450 The raw sequence reads have been deposited into the DNA Data Bank of Japan (DDBJ)
451 Sequence Read Archive database under the accession number DRA012420 for ITS1 and
452 DRA012422 for ITS2. OTU sequences were registered as LC602782 - LC602786 for
453 *Ceratobasidium,* LC602787 - LC602792 for *Serendipita*, and LC602793 - LC602794 for
454 *Tulasnella.* ITS sequences of isolated *Ceratobasidium* were registered as LC600231for BI-
455 103P and LC600232 for DE-52P.
456
457 **Author Contributions**

458 GCP, CM, MY, and HK designed the experiments; GCP and IN performed the experiments
459 and analyzed the sequencing data; GCP, CM, MY, and HK wrote the manuscript. All authors
460 approved the final manuscript.
461

462 **Acknowledgments**

463 We are grateful to the Japanese Ministry of Education, Culture, Sports, Science, and
464 Technology (MEXT) scholarship to GCP and Research Fellowships of Japan Society for the
465 Promotion of Science (JSPS) for Young Scientists (grant number 201801755) to CM. We also
466 thank Takahiro Yagame (Mizuho Kyodo Museum) for the provision of *Ceratobasidium* TA1-
467 1 and TA2-1, Kenji Suetsugu (Kobe University) for the critical reading of the manuscript, and
468 Rudy Hermawan (Tottori University) for technical assistance.
469

470 **Conflict of interest**

471 The authors declare no competing interests.
472

References

Almeida PRM, van den Berg C, Góes-Neto A (2014) *Epulorhiza amonilioides* sp. nov.: a new anamorphic species of orchid mycorrhiza from Brazil. Neodiversity 7:1–10. https://doi.org/10.13102/neod.71.1

Arditti J, Ghani AKA (2000) Numerical and physical properties of orchid seeds and their biological implications. New Phytologist 145:367–421. https://doi.org/10.1046/j.1469-8137.2000.00587.x

Barthlott W, Große-Veldmann B, Korotkova N (2014) Orchid seed diversity: A scanning electron microscopy survey. Englera, Berlin. ISBN: 9783921800928

Bolyen E, Rideout JR, Dillon MR, et al (2019) Reproducible, interactive, scalable and extensible microbiome data science using QIIME 2. Nature Biotechnology 37:852–857. https://doi.org/10.1038/s41587-019-0209-9

Carlsward BS, Whitten WM, Williams NH, Bytebier B (2006) Molecular phylogenetics of Vandeae (Orchidaceae) and the evolution of leaflessness. American Journal of Botany 93:770–786. https://doi.org/10.3732/ajb.93.5.770

Chomicki G, Bidel LPR, Jay-Allemand C (2014) Exodermis structure controls fungal invasion in the leafless epiphytic orchid *Dendrophylax lindenii* (Lindl.) Benth. ex Rolfe. Flora 209:88–94. https://doi.org/10.1016/j.flora.2014.01.001

Clarke KR (1993) Non-parametric multivariate analysis of changes in community structure. Australian Journal of Ecology 18:117–143. https://doi.org 10.1111/j.1442-9993.1993.tb00438.x

494 Esnault A-L, Masuhara G, McGee PA (1994) Involvement of exodermal passage cells in
495 mycorrhizal infection of some orchids. Mycological Research 98:672–676.
496 https://doi.org/10.1016/S0953-7562(09)80415-2

497 Freitas EFS, da Silva M, Cruz E da S, et al (2020) Diversity of mycorrhizal *Tulasnella*
498 associated with epiphytic and rupicolous orchids from the Brazilian Atlantic Forest,
499 including four new species. Scientific Reports 10:7069. https://doi.org/10.1038/s41598-
500 020-63885-w

501 Gange AC, Bower E, Stagg PG, et al (1999) A comparison of visualization techniques for
502 recording arbuscular mycorrhizal colonization. New Phytologist 142: 123-132.
503 https://doi.org /10.1046/j.1469-8137.1999.00371.x

504 Guimarães FAR, Pereira MC, Felício C da S, et al (2013) Symbiotic propagation of seedlings
505 of *Cyrtopodium glutiniferum* Raddi (Orchidaceae). Acta Botanica Brasilica 27:590–596.
506 https://doi.org/10.1590/S0102-33062013000300016

507 Hannon GJ (2010) FASTX-Toolkit.

508 Herrera P, Suárez JP, Kottke I (2010) Orchids keep the ascomycetes outside: a highly diverse
509 group of ascomycetes colonizing the velamen of epiphytic orchids from a tropical
510 mountain rainforest in Southern Ecuador. Mycology 1:262–268.
511 https://doi.org/10.1080/21501203.2010.526645

512 Hoang NH, Kane ME, Radcliffe EN, et al (2017) Comparative seed germination and seedling
513 development of the ghost orchid, *Dendrophylax lindenii* (Orchidaceae), and molecular
514 identification of its mycorrhizal fungus from South Florida. Annals of Botany 119:379–
515 393. https://doi.org/10.1093/aob/mcw220

516 Ihrmark K, Bödeker ITM, Cruz-Martinez K, et al (2012) New primers to amplify the fungal
517 ITS2 region - evaluation by 454-sequencing of artificial and natural communities. FEMS
518 Microbiology Ecology 82:666–677. https://doi.org/10.1111/j.1574-6941.2012.01437.x

519 Inglis PW, Marilia de Castro RP, Resende L V., Grattapaglia D (2018) Fast and inexpensive
520 protocols for consistent extraction of high quality DNA and RNA from challenging plant
521 and fungal samples for high-throughput SNP genotyping and sequencing applications.
522 PLoS ONE 13:1–14. https://doi.org/10.1371/journal.pone.0206085

523 Joshi N, Fass JN (2011) Sickle: A sliding-window, adaptive, quality-based trimming tool for
524 FastQ files (Version 1.33). Available at https://github.com/najoshi/sickle.

525 Kassambara A (2018) ggpubr: "ggplot2" Based Publication Ready Plots. R package version
526 0.2. Available at https://CRAN.R-project.org/package=ggpubr.

527 Kendon JP, Yokoya K, Zettler LW, et al (2020) Recovery of mycorrhizal fungi from wild
528 collected protocorms of Madagascan endemic orchid *Aerangis ellisii* (B.S. Williams)
529 Schltr. and their use in seed germination in vitro. Mycorrhiza 30:567-576.
530 https://doi.org/10.1007/s00572-020-00971-x

531 Kuga Y, Sakamoto N, Yurimoto H (2014) Stable isotope cellular imaging reveals that both
532 live and degenerating fungal pelotons transfer carbon and nitrogen to orchid protocorms.
533 New Phytologist 202:594–605. https://doi.org/10.1111/nph.12700

534 Magoč T, Salzberg SL (2011) FLASH: Fast length adjustment of short reads to improve
535 genome assemblies. Bioinformatics 27:2957–2963.
536 https://doi.org/10.1093/bioinformatics/btr507

537 Moore RM, Harrison AO, McAllister SM, et al (2020) Iroki: automatic customization and
538 visualization of phylogenetic trees. PeerJ 8:e8584. https://doi.org/10.7717/peerj.8584

539 Mújica EB, Mably JJ, Skarha SM, et al (2018) A comparision of ghost orchid (*Dendrophylax*
540 *lindenii*) habitats in Florida and Cuba, with particular reference to seedling recruitment
541 and mycorrhizal fungi. Botanical Journal of the Linnean Society 186:572–586.
542 https://doi.org/10.1093/botlinnean/box106

543 Naranjo-Ortiz MA, Gabaldón T (2019) Fungal evolution: major ecological adaptations and
544 evolutionary transitions. Biological Reviews 94:1443–1476.
545 https://doi.org/10.1111/brv.12510

546 Nilsson RH, Larsson KH, Taylor AFS, et al (2019) The UNITE database for molecular
547 identification of fungi: Handling dark taxa and parallel taxonomic classifications.
548 Nucleic Acids Research 47:D259–D264. https://doi.org/10.1093/nar/gky1022

549 Oberwinkler F, Riess K, Bauer R, et al (2013) Taxonomic re-evaluation of the
550 *Ceratobasidium-Rhizoctonia* complex and *Rhizoctonia butinii*, a new species attacking
551 spruce. Mycological Progress 12:763–776. https://doi.org/10.1007/s11557-013-0936-0

552 Ogle DH, Wheeler P, Dinno A (2021) FSA: Fisheries Stock Analysis. R package version
553 0.9.1.9000. Available at https://github.com/droglenc/FSA.

554 Ogoshi A (1975) Studies on the anastomosis groups of *Rhizoctonia solani* Kühn. Bull Natl
555 Inst, Agrie Sci Ser C 9:198–203

556 Oksanen J, Legendre P, O'Hara B, et al (2007) The vegan package. Community ecology
557 package 10:631–637. Available at http://vegan.r-forge.r-project.org/

558 Otero JT, Ackerman JD, Bayman P (2002) Diversity and host specificity of endophytic
559 *Rhizoctonia*-like fungi from tropical orchids. American Journal of Botany 89:1852–1858.
560 https://doi.org/10.3732/ajb.89.11.1852

561 Pujasatria GC, Miura C, Kaminaka H (2020) In vitro symbiotic germination: A revitalized
562 heuristic approach for orchid species conservation. Plants 9:1–15.
563 https://doi.org/10.3390/plants9121742

564 Rachanarin C, Suwannarach N, Kumla J, et al (2018) A new endophytic fungus, *Tulasnella*
565 *phuhinrongklaensis* (Cantharellales, Basidiomycota) isolated from roots of the terrestrial
566 orchid, *Phalaenopsis pulcherrima*. Phytotaxa 374:99–109.
567 https://doi.org/10.11646/phytotaxa.374.2.1

568 Rammitsu K, Kajita T, Imai R, Ogura-Tsujita Y (2021) Strong primer bias for Tulasnellaceae
569 fungi in metabarcoding: Specific primers improve the characterization of the mycorrhizal
570 communities of epiphytic orchids. Mycoscience 62:1–17.
571 https://doi.org/10.47371/mycosci.2021.06.005

572 Rammitsu K, Yagame T, Yamashita Y, et al (2019) A leafless epiphytic orchid,
573 *Taeniophyllum glandulosum* Blume (Orchidaceae), is specifically associated with the
574 Ceratobasidiaceae family of basidiomycetous fungi. Mycorrhiza 29:159–166.
575 https://doi.org/10.1007/s00572-019-00881-7

576 Rasmussen HN, Dixon KW, Jersáková J, Těšitelová T (2015) Germination and seedling
577 establishment in orchids: A complex of requirements. Annals of Botany 116:391–402.
578 https://doi.org/10.1093/aob/mcv087

579 Rasmussen HN, Rasmussen FN (2018) The epiphytic habitat on a living host: Reflections on
580 the orchid-tree relationship. Botanical Journal of the Linnean Society 186:456–472.
581 https://doi.org/10.1093/botlinnean/box085

582 Riess K, Oberwinkler F, Bauer R, Garnica S (2014) Communities of endophytic Sebacinales
583 associated with roots of herbaceous plants in agricultural and grassland ecosystems are
584 dominated by *Serendipita herbamans* sp. nov. PLoS ONE 9: e94676.
585 https://doi.org/10.1371/journal.pone.0094676

586 Sarsaiya S, Jain A, Jia Q, et al (2020) Molecular identification of endophytic fungi and their
587 pathogenicity evaluation against *Dendrobium nobile* and *Dendrobium officinale.*
588 International Journal of Molecular Sciences 21:1–16.
589 https://doi.org/10.3390/ijms21010316

590 Schoch CL, Sung GH, López-Giráldez F, et al (2009) The Ascomycota tree of life: A phylum-
591 wide phylogeny clarifies the origin and evolution of fundamental reproductive and
592 ecological traits. Systematic Biology 58:224–239. https://doi.org/10.1093/sysbio/syp020

593 Singh US, Kumar J (1991) Staining of nuclei in fungi by ethidium bromide. Biotechnic and
594 Histochemistry 66:266–268. https://doi.org/10.3109/10520299109109984

595 Suetsugu K, Tanaka K, Okuyama Y, Yukawa T (2015) Potential pollinator of *Vanda falcata*
596 (Orchidaceae): *Theretra* (Lepidoptera: Sphingidae) hawkmoths are visitors of long
597 spurred orchid. European Journal of Entomology 112:393–397.
598 https://doi.org/10.14411/eje.2015.031

599 Taylor DL, McCormick MK (2008) Internal transcribed spacer primers and sequences for
600 improved characterization of basidiomycetous orchid mycorrhizas. New Phytologist
601 177:1020–1033. https://doi.org/10.1111/j.1469-8137.2007.02320.x

602 Toju H, Tanabe AS, Yamamoto S, Sato H (2012) High-coverage ITS primers for the DNA-
603 based identification of ascomycetes and basidiomycetes in environmental samples. PLoS
604 ONE 7: e40863. https://doi.org/10.1371/journal.pone.0040863

605 Warcup JH, Talbot PHB (1980) Perfect States of Rhizoctonias Associated With Orchids. Iii.
606 New Phytologist 86:267–272. https://doi.org/10.1111/j.1469-8137.1980.tb00787.x

607 Weiß M, Waller F, Zuccaro A, Selosse MA (2016) Sebacinales - one thousand and one
608 interactions with land plants. New Phytologist 211:20–40.
609 https://doi.org/10.1111/nph.13977

610 Xing X, Jacquemyn H, Gai X, et al (2019) The impact of life form on the architecture of
611 orchid mycorrhizal networks in tropical forest. Oikos 128:1254–1264.
612 https://doi.org/10.1111/oik.06363

613 Yang RH, Su JH, Shang JJ, et al (2018) Evaluation of the ribosomal DNA internal transcribed
614 spacer (ITS), specifically ITS1 and ITS2, for the analysis of fungal diversity by deep
615 sequencing. PLoS ONE 13:1–17. https://doi.org/10.1371/journal.pone.0206428

616 Yeh CM, Chung KM, Liang CK, Tsai WC (2019) New insights into the symbiotic
617 relationship between orchids and fungi. Applied Sciences 9:1–14.
618 https://doi.org/10.3390/app9030585

619 Yukawa T, Ogura-Tsujita Y, Shefferson RP, Yokoyama J (2009) Mycorrhizal diversity in
620 *Apostasia* (Orchidaceae)indicates the origin and evolution of orchid mycorrhiza.
621 American Journal of Botany 96:1997–2009. https://doi.org/10.3732/ajb.0900101

622 Zettler LW, Corey LL, Jacks AL, et al (2013) *Tulasnella irregularis* (Basidiomycota:
623 Tulasnellaceae) from roots of *Encyclia tampensis* in South Florida, and confirmation of
624 its mycorrhizal significance through symbiotic seed germination. Lankesteriana 13:119–
625 128. https://doi.org/10.15517/lank.v0i0.11552

626 Zettler LW, Poulter SB, McDonald KI, Stewart SL (2007) Conservation-driven propagation
627 of an epiphytic orchid (*Epidendrum nocturnum*) with a mycorrhizal fungus. HortScience
628 42: 135-139. https://doi.org/10.21273/hortsci.42.1.135

629 Zhang Y, Crous PW, Schoch CL, Hyde KD (2012) Pleosporales. Fungal Diversity 53:1–221.
630 https://doi.org/10.1007/s13225-011-0117-x

631

632

633 **Figure legends**

634 **Fig. 1.** Plant samples. A) Location of Mie Prefecture, Kihoku Town, and Suzuka City (green)
635 inside Japan. B) *Vanda falcata* young plant example. C) Adult plants with old, drying
636 inflorescences. D) Colonized root parts conspicuously turned yellow upon orchid mycorrhizal
637 fungi (OMF) colonization (arrowheads). E) OMF mostly colonizes the root part that attaches
638 to the bark. Bar = 1-mm.

639

640 **Fig. 2.** Beta diversity of the fungi in *Vanda falcata* based on the ITS1 and ITS2 sequences.
641 Principal coordinate analysis (PCoA) plots of ITS1 (A) and ITS2 (B) based on Bray-Curtis
642 distance showing a composition of fungal community structure in all samples, e.g., seeds
643 from seed baiting (SB, red), young plant roots (YR, green), and adult plant roots (AR, blue).
644 R-value was calculated using ANOSIM ($p < 0.05$).

645

646 **Fig. 3.** *Rhizoctonia*-like fungal OTUs inferred from amplicon sequencing results. A) Heat
647 map diagram showing *Rhizoctonia*-like fungi OTUs present in seed (SB), seedling (Y1-3),
648 and adult (A1-4) root samples. B) Maximum likelihood (ML) phylogenetic tree of OTUs
649 assigned to each order (colored branches)–Cantharellales (chartreuse) and Sebacinales (light
650 blue)–and family (arcs): Ceratobasidiaceae (green), Serendipitaceae (blue), Sebacinaceae
651 (light blue), and Tulasnellaceae (yellow). Only bootstrap numbers above 80% (dotted nodes)
652 are shown. *Clavulina caespitosa, Craterellus atratoides,* and *Craterellus indicus* are used as
653 outgroups from Cantharellales.

654

655 **Fig. 4.** Colonization of ascomycetous and orchid mycorrhizal fungi (OMF) inside roots. A)
656 Conidia of *Lasiodiplodia* (L) and unidentified Pleosporales (P) on the epidermis. B) OMF

hyphae (arrowheads) infiltrating the cortical cells (Co) through velamen (VR) and passage cell (PC) of exodermis (Ex). Bar = 40 μm. C) Localization of exodermal passage cells in the upper, side, and lower parts of root (left), and those colonized by OMF (right). Different letters represent significant difference by Tukey's test at $p < 0.05$.

Fig. 5. *In vitro* germination assay results. *Vanda falcata* seeds were inoculated with eleven *Rhizoctonia*-like fungi, including those isolated in this study (BI-103P and DE-52P). Boxplots showing growth index (A) and symbiotic cell count (B) after eight weeks. Different letters represent significant difference by Dunn's test at $p < 0.05$.

Fig. 6. Maximum likelihood phylogenetic tree of *Ceratobasidium* strains, including those inducing seed germination of *Vanda falcata* (red) and other isolated strains (blue). Dotted nodes indicate a bootstrap number of 80% or higher. The clade containing strains with the best germination output is shown in chartreuse branches. Adjacent boxes indicate the nutritional mode of each species, i.e., plant-pathogen (red), saprobe (yellow), orchid mycorrhizal fungus (green), and lichen-forming (blue). *Rhizoctonia solani* strains are used as an outgroup (red branches).

Fig. 7. Infected *Vanda falcata* seeds upon inoculation with pathogenic ascomycetous fungi isolated from *V. falcata* roots. A) Seeds infected with *Pyrenochaetopsis.* Black, swollen seed (arrow) was filled with pycnidium. (B) Seed colonized by *Fusarium.* Although inconspicuous, the seed starts to degrade.

680 **Fig. 8**. Inner fungal community composition in *Vanda falcata.* Along with growth and
681 development (i.e., from seed germination to reproductive stage), despite an increase in size
682 and trophic mode, the inner fungal community has a similar structure with Ascomycota as the
683 dominant phylum, followed by Basidiomycota. Even for Basidiomycota, *Rhizoctonia*-like
684 fungi abundance is less than half compared to other genera. Among all *Rhizoctonia*-like fungi,
685 *Ceratobasidium* is the OMF of *V. falcata* based on germination assay results, thus correlating
686 with its higher portion. Additionally, only *Rhizoctonia*-like fungus colonizes cortical cells
687 through exodermal passage cells.
688

689 **Table 1.** *Rhizoctonia*-like fungi used for *Vanda falcata* seed symbiotic germination

Treatment	Species name	Strain no.	Source	
			Host plant	Location
C.gra53	*Ceratobasidium gramineum*	MAFF235853	*Agrostis sp.* * **	Japan
C.sp.87	*Ceratobasidium sp.*	MAFF244587	*Dactylorhiza aristata*	Japan
C.sp.BI	*Ceratobasidium sp.*	N/A	this study	Japan
C.sp.DE	*Ceratobasidium sp.*	N/A	this study	Japan
C.sp.TA1	*Ceratobasidium sp.*	NBRC109234	*Taeniophyllum glandulosum*	Japan
C.sp.TA2	*Ceratobasidium sp.*	NBRC109235	*Taeniophyllum glandulosum*	Japan
S.ind27	*Serendipita indica*	ATCC DSM11827	*Prosopis juliflora* and *Zizyphus nummularia** ***	India
S.ver30	*Serendipita vermifera*	MAFF305830	*Cyrtostylis reniformis*	Australia
T.asy08	*Tulasnella asymmetrica*	MAFF305808	*Thelymitra epipactoides*	Australia
T.cal05	*Tulasnella calospora*	MAFF305805	unspecified	Australia
T.irr96	*Tulasnella irregularis*	JCM9996	*Dendrobium dicuphum*	Australia

* Non-orchidaceous plants, ** isolated as pathogen, *** isolated as endophyte

690

691 **Table 2.** Seed germination stage morphological descriptions

Stage	Description
0	No response
1	Imbibition, OMF starts to colonize
2	Swelling, testa rupture, formation of rhizoids
3	Formation of shoot primordium
4	Formation of first crest
5	Formation of first leaf

692

693 **Table 3.** Isolated fungi from *Vanda falcata* seedling and adult plant roots

Isolate	Source sample	Closest match in Genbank	Similarity
BI-103P	Young root	AB507066.1 uncultured Ceratobasidiaceae from *Sedirea japonica* (Miyazaki Prefecture, Japan)	97.74%
DE-52P	Adult plant root	AB507066.1 uncultured Ceratobasidiaceae from *Sedirea japonica* (Miyazaki Prefecture, Japan)	98.79%
MI-3	Young root	NR_155625.1 *Parateratosphaeria karinae* holotype CBS128774 (South Africa)	84.20%
MI-4	Young root	NR_153559.1 *Atrocalyx bambusae* holotype MFLU 11-0150 (Thailand)	97.25%
MI-5	Young root	NR_159064.1 *Subulicystidium harpagum* isotype KAS L 1726a (Réunion Island)	89.26%
NE-4	Adult plant root	NR_160059.1 *Pyrenochaetopsis microspora* type material CBS 102876 (Montenegro)	99.81%
NE-5	Adult plant root	NR_137617.1 *Fusicolla violacea* holotype CBS:634.76 (Iran)	80.92%

694

Fig. 1

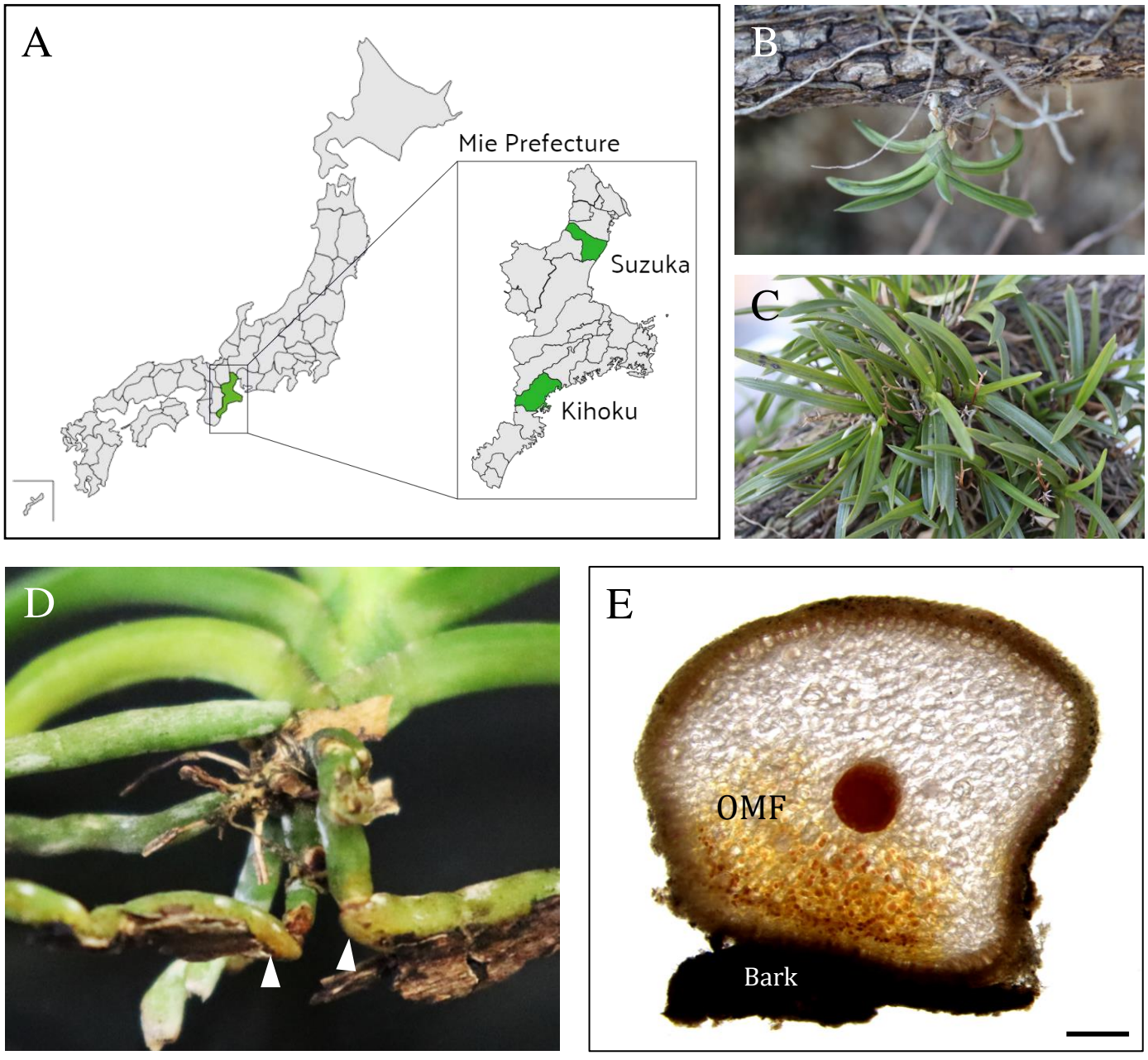

Fig. 2

A

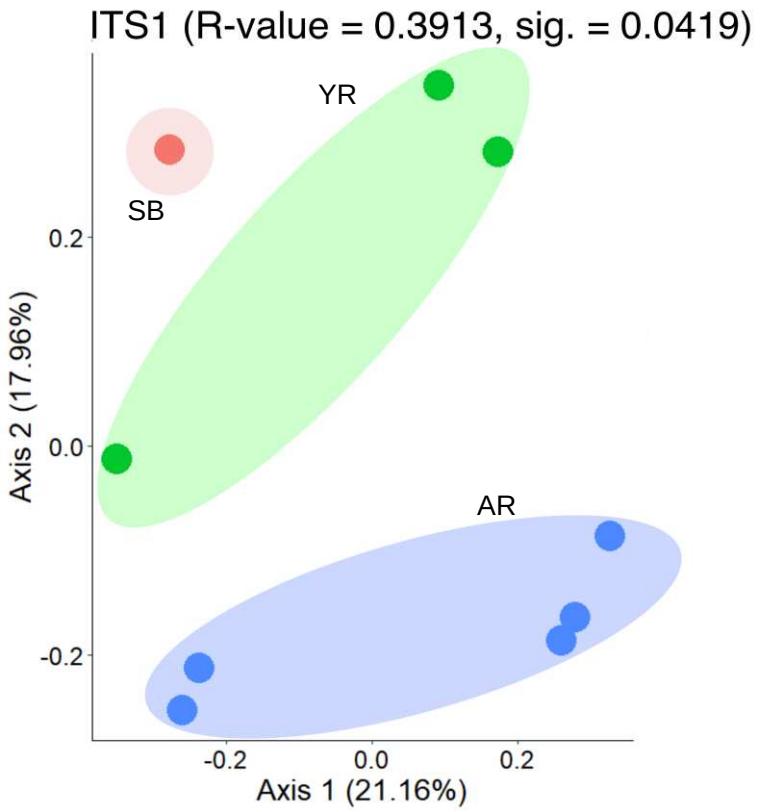
ITS1 (R-value = 0.3913, sig. = 0.0419)
YR
SB
AR
0.2
0.0
-0.2
Axis 2 (17.96%)
-0.2
0.0
0.2
Axis 1 (21.16%)

B

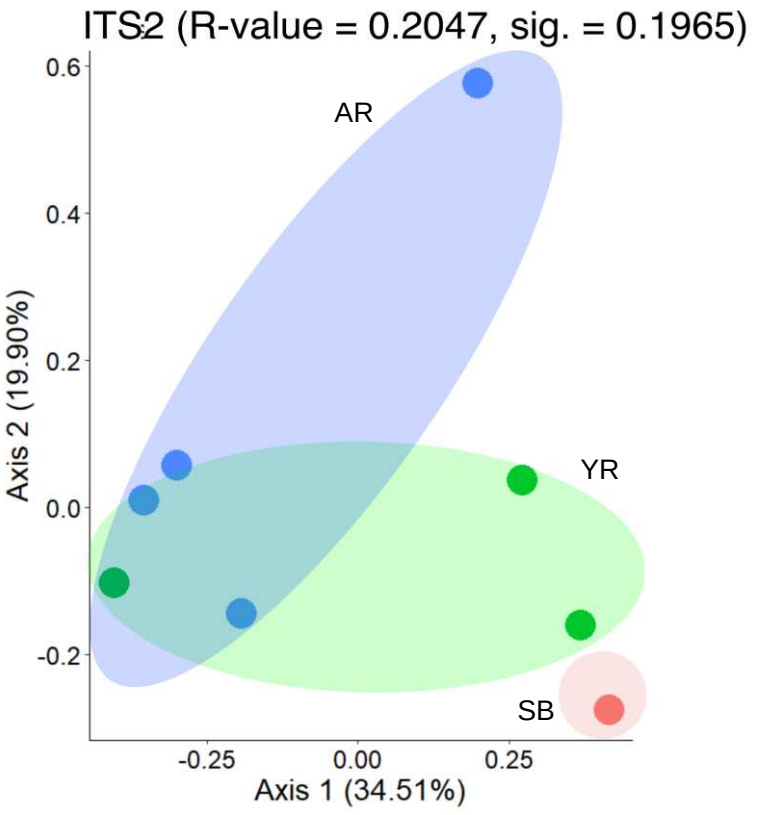
ITS2 (R-value = 0.2047, sig. = 0.1965)
AR
YR
SB
0.6
0.4
0.2
0.0
-0.2
Axis 2 (19.90%)
-0.25
0.00
0.25
Axis 1 (34.51%)

Fig. 3

A

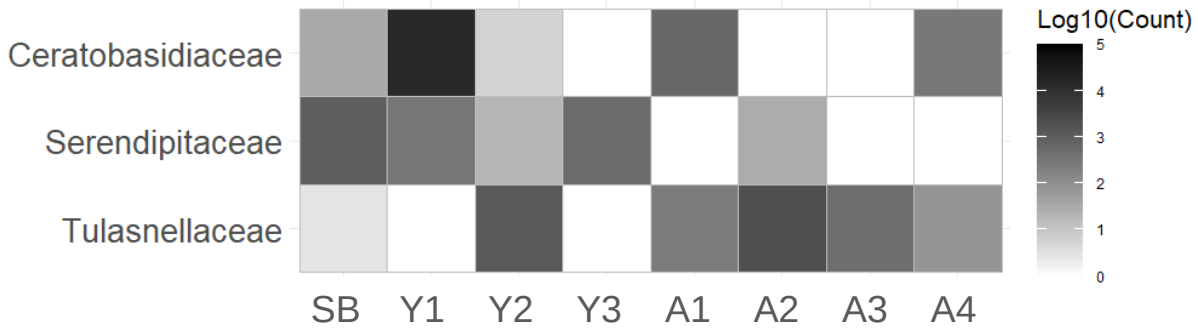
Ceratobasidiaceae
Serendipitaceae
Tulasnellaceae
SB
Y1
Y2
Y3
A1
A2
A3
A4
Log10(Count)
5
4
3
2
1
0

B

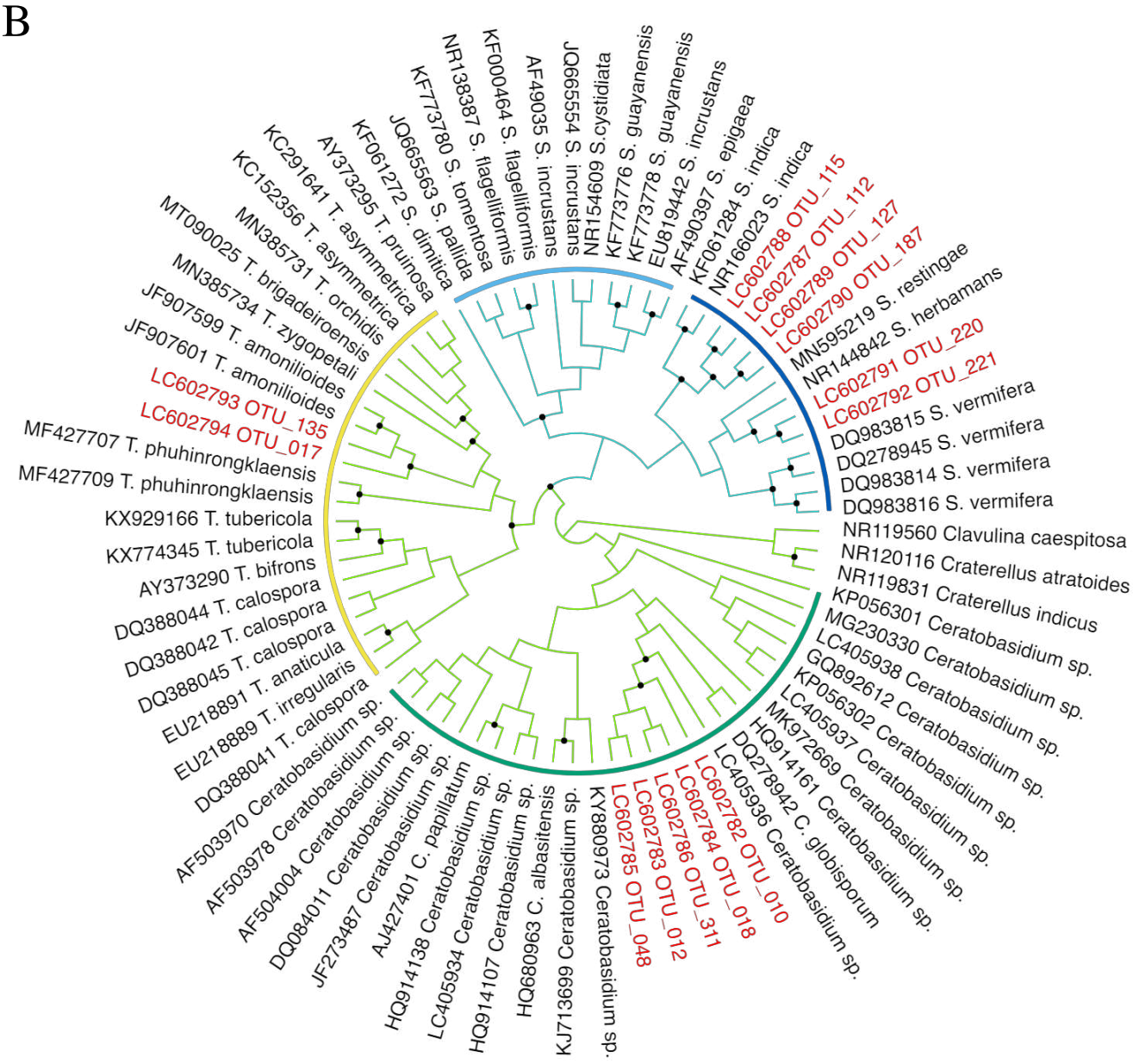
KF000464 S. flagelliformis
NR138387 S. flagelliformis
AF49035 S. incrustans
JQ665554 S. incrustans
NR154609 S.cystidiata
KF773776 S. guayanensis
KF773778 S. guayanensis
EU819442 S. incrustans
AF490397 S. epigaea
KF061284 S. indica
NR166023 S. indica
KF773780 S. tomentosa
JQ665563 S. pallida
KF061272 S. dimitica
AY373295 T. pruinosa
KC291641 T. asymmetrica
KC152356 T. asymmetrica
MN385731 T. orchidis
MT090025 T. brigadeiroensis
JF907599 T. zygopetali
MN385734 T. amonilioides
JF907601 T. amonilioides
LC602793 OTU_135
LC602794 OTU_017
MF427707 T. phuhinrongklaensis
MF427709 T. phuhinrongklaensis
KX929166 T. tubericola
KX774345 T. tubericola
AY373290 T. bifrons
DQ388044 T. calospora
DQ388042 T. calospora
DQ388045 T. calospora
EU218891 T. anaticula
EU218889 T. irregularis
DQ388041 T. calospora
AF503970 Ceratobasidium sp.
AF503978 Ceratobasidium sp.
AF504004 Ceratobasidium sp.
DQ084011 Ceratobasidium sp.
JF273487 Ceratobasidium sp.
AJ427401 C. papillatum
HQ914138 Ceratobasidium sp.
LC405934 Ceratobasidium sp.
HQ914107 Ceratobasidium sp.
HQ680963 C. albasitensis
KJ713699 Ceratobasidium sp.
KY880973 Ceratobasidium sp.
LC602785 OTU_048
LC602783 OTU_012
LC602786 OTU_311
LC602784 OTU_018
LC602782 OTU_010
LC405936 Ceratobasidium sp.
DQ278942 C. globisporum
HQ914161 Ceratobasidium sp.
MK972669 Ceratobasidium sp.
LC405937 Ceratobasidium sp.
KP056302 Ceratobasidium sp.
GQ892612 Ceratobasidium sp.
LC405938 Ceratobasidium sp.
MG230330 Ceratobasidium sp.
KP056301 Ceratobasidium sp.
NR119831 Craterellus indicus
NR120116 Craterellus atratoides
NR119560 Clavulina caespitosa
DQ983816 S. vermifera
DQ983814 S. vermifera
DQ278945 S. vermifera
DQ983815 S. vermifera
LC602792 OTU_221
LC602791 OTU_220
NR144842 S. herbamans
MN595219 S. restingae
LC602790 OTU_187
LC602789 OTU_127
LC602787 OTU_112
LC602788 OTU_115

Fig. 4

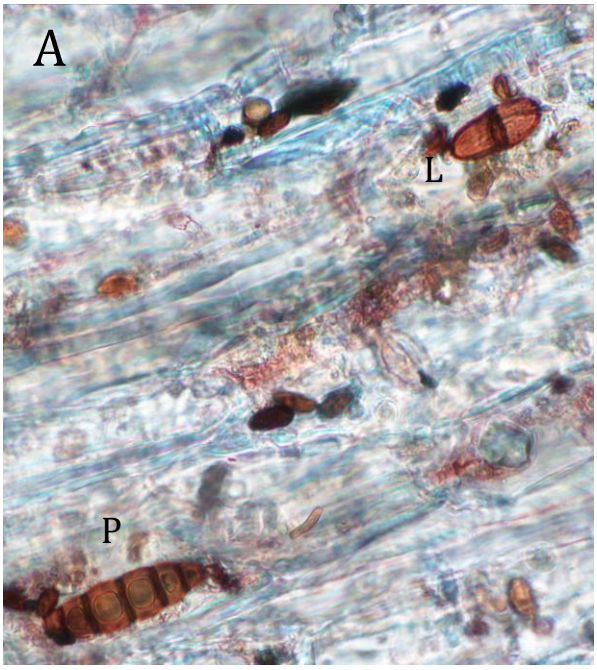
A
L
P

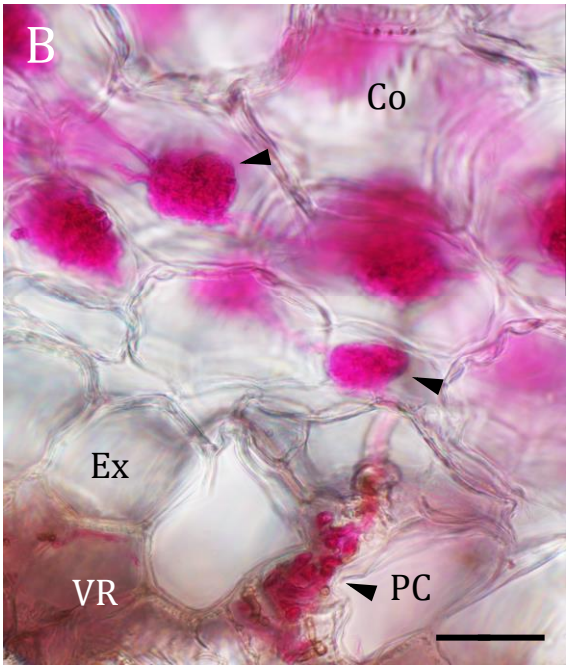
B
Co
Ex
VR
PC

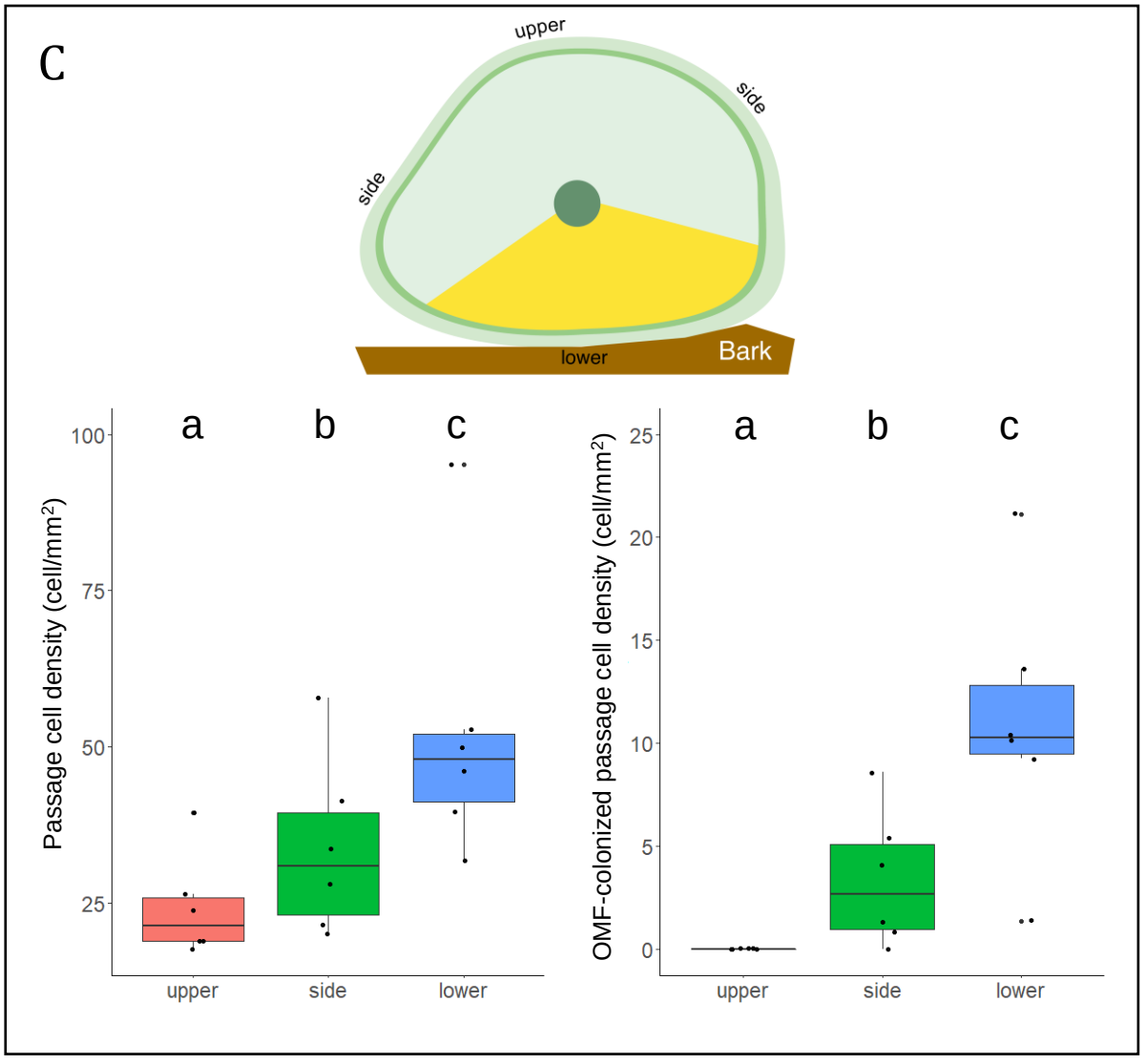
C
upper
side
side
lower
Bark
a
b
c
Passage cell density (cell/mm²)
100
75
50
25
upper
side
lower
a
b
c
OMF-colonized passage cell density (cell/mm²)
25
20
15
10
5
0
upper
side
lower

Fig. 5

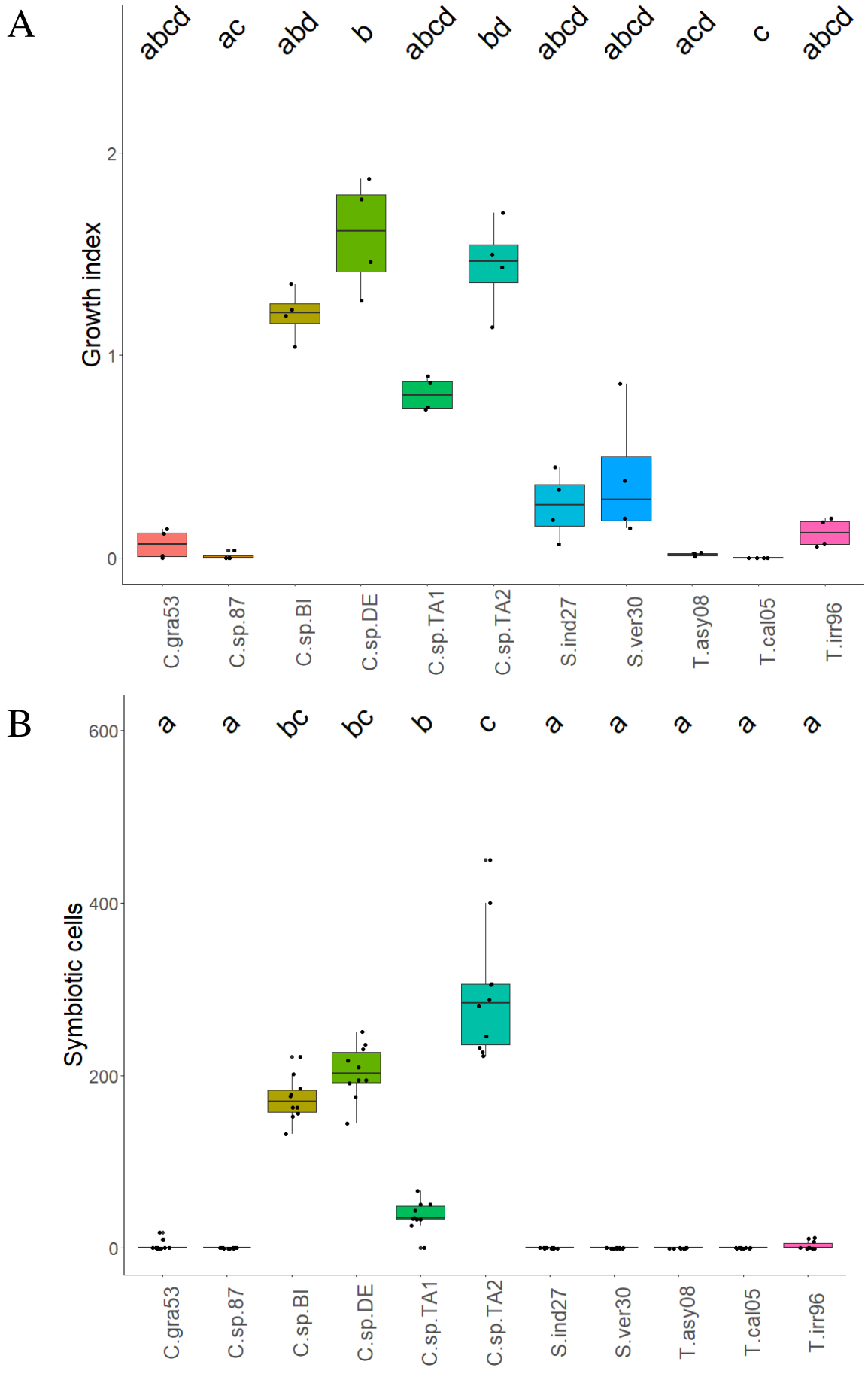
A
abcd
ac
abd
b
abcd
bd
abcd
abcd
acd
c
abcd
Growth index
0
1
2
C.gra53
C.sp.87
C.sp.BI
C.sp.DE
C.sp.TA1
C.sp.TA2
S.ind27
S.ver30
T.asy08
T.cal05
T.irr96
B
a
a
bc
bc
b
c
a
a
a
a
a
Symbiotic cells
0
200
400
600
C.gra53
C.sp.87
C.sp.BI
C.sp.DE
C.sp.TA1
C.sp.TA2
S.ind27
S.ver30
T.asy08
T.cal05
T.irr96

Fig. 6

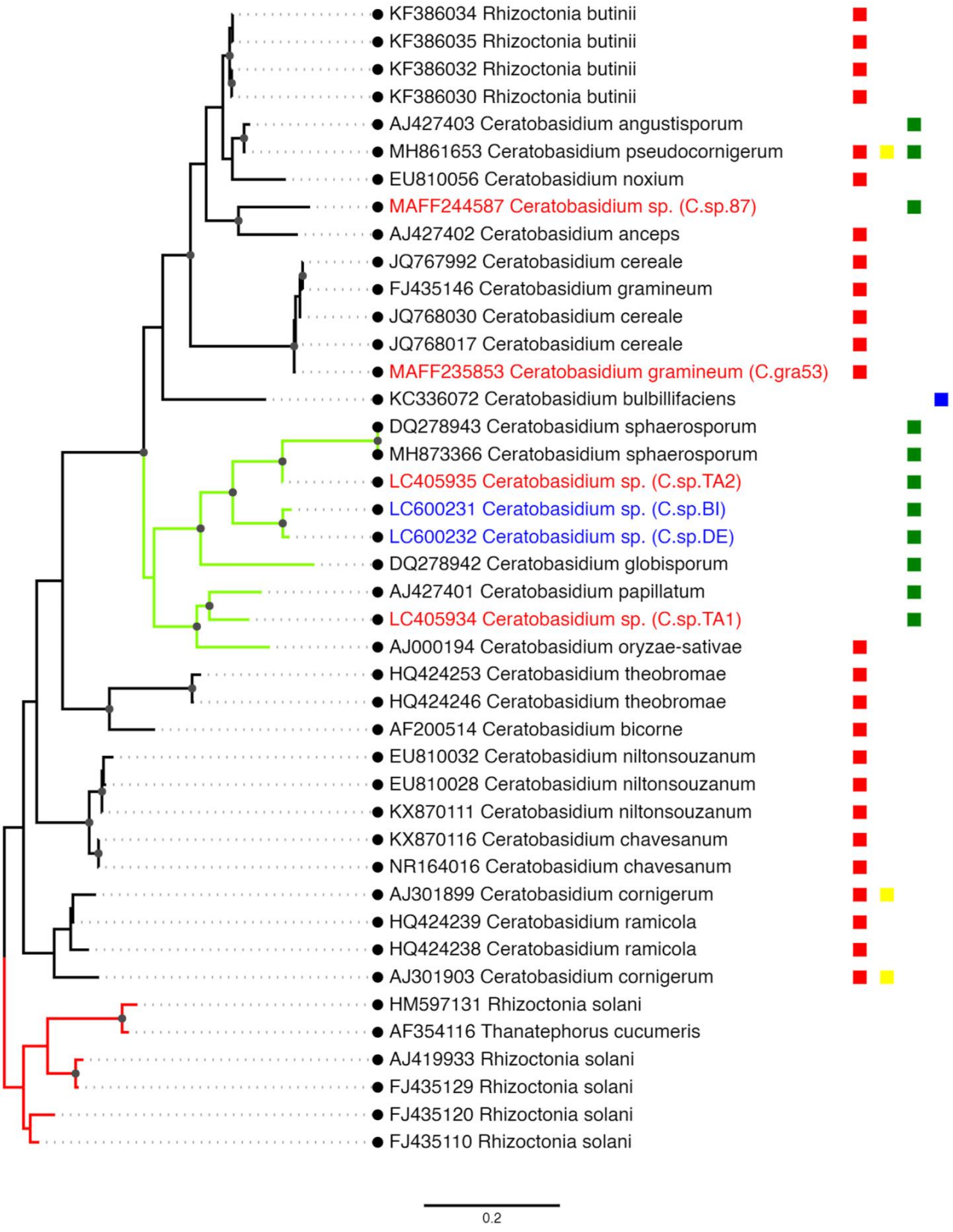
KF386034 Rhizoctonia butinii
KF386035 Rhizoctonia butinii
KF386032 Rhizoctonia butinii
KF386030 Rhizoctonia butinii
AJ427403 Ceratobasidium angustisporum
MH861653 Ceratobasidium pseudocornigerum
EU810056 Ceratobasidium noxium
MAFF244587 Ceratobasidium sp. (C.sp.87)
AJ427402 Ceratobasidium anceps
JQ767992 Ceratobasidium cereale
FJ435146 Ceratobasidium gramineum
JQ768030 Ceratobasidium cereale
JQ768017 Ceratobasidium cereale
MAFF235853 Ceratobasidium gramineum (C.gra53)
KC336072 Ceratobasidium bulbillifaciens
DQ278943 Ceratobasidium sphaerosporum
MH873366 Ceratobasidium sphaerosporum
LC405935 Ceratobasidium sp. (C.sp.TA2)
LC600231 Ceratobasidium sp. (C.sp.BI)
LC600232 Ceratobasidium sp. (C.sp.DE)
DQ278942 Ceratobasidium globisporum
AJ427401 Ceratobasidium papillatum
LC405934 Ceratobasidium sp. (C.sp.TA1)
AJ000194 Ceratobasidium oryzae-sativae
HQ424253 Ceratobasidium theobromae
HQ424246 Ceratobasidium theobromae
AF200514 Ceratobasidium bicorne
EU810032 Ceratobasidium niltonsouzanum
EU810028 Ceratobasidium niltonsouzanum
KX870111 Ceratobasidium niltonsouzanum
KX870116 Ceratobasidium chavesanum
NR164016 Ceratobasidium chavesanum
AJ301899 Ceratobasidium cornigerum
HQ424239 Ceratobasidium ramicola
HQ424238 Ceratobasidium ramicola
AJ301903 Ceratobasidium cornigerum
HM597131 Rhizoctonia solani
AF354116 Thanatephorus cucumeris
AJ419933 Rhizoctonia solani
FJ435129 Rhizoctonia solani
FJ435120 Rhizoctonia solani
FJ435110 Rhizoctonia solani
0.2

Fig. 7

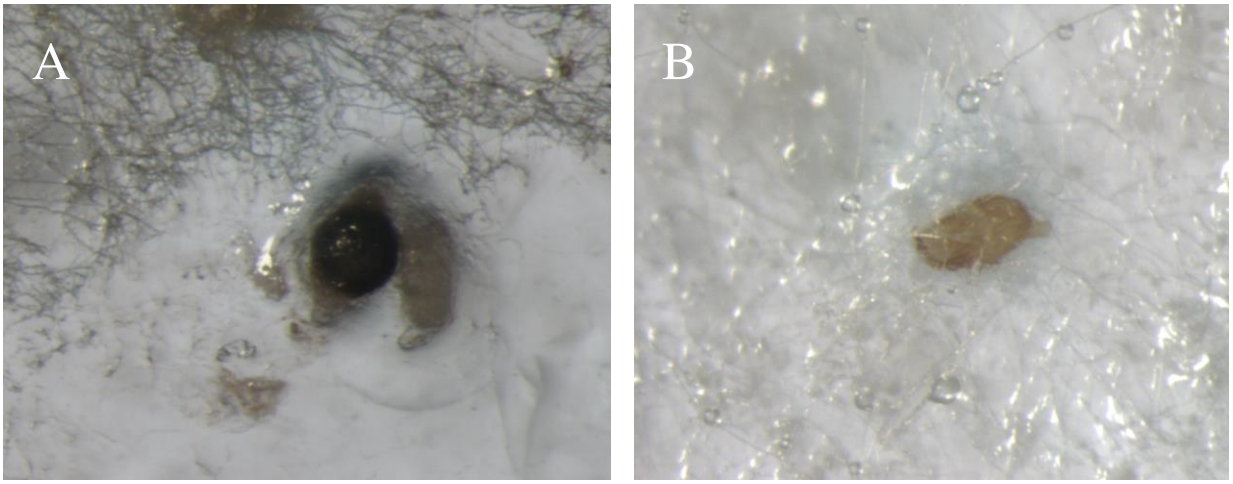

Fig. 8

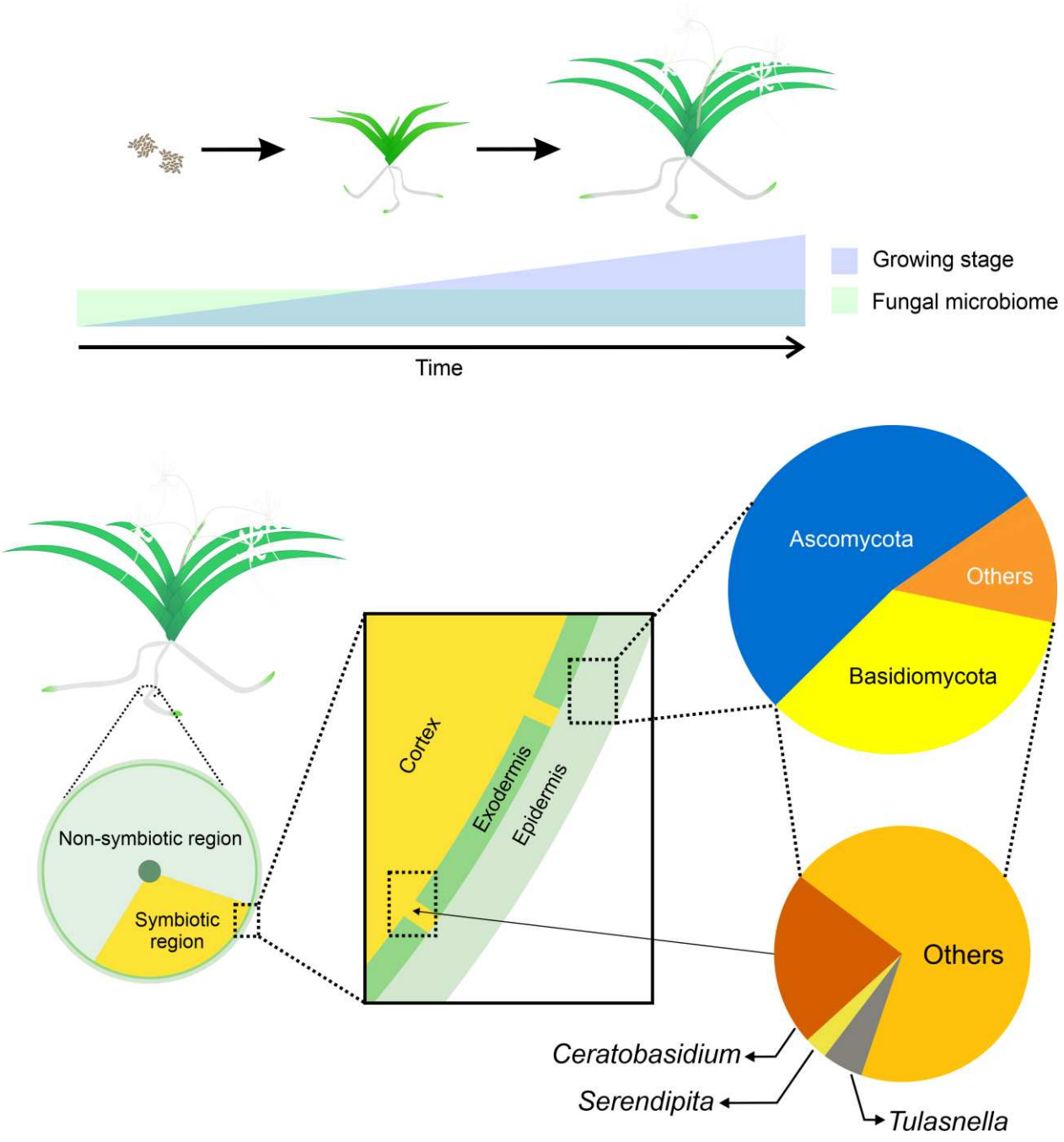
Growing stage
Fungal microbiome
Time
Non-symbiotic region
Symbiotic region
Cortex
Exodermis
Epidermis
Ascomycota
Others
Basidiomycota
Others
Ceratobasidium
Serendipita
Tulasnella